SYNTHESIS OF GRAPHENE QUANTUM DOTS (GQDs) FROM PADDY STRAW FOR BILIRUBIN DETECTION

A DISSERTATION

SUBMITTED IN PARTIAL FULFILLMENT OF THE REQUIREMENTS

FOR THE AWARD OF THE DEGREE

OF

MASTER OF SCIENCE

IN

PHYSICS

Submitted by:

ISHA

(2K22/MSCPHY/14)

Under the supervision of

DR. MOHAN SINGH MEHATA

DEPARTMENT OF APPLIED PHYSICS
DELHI TECHNOLOGICAL UNIVERSITY
(Formerly Delhi College of Engineering)
Bawana Road, Delhi – 110042

JUNE, 2024

CANDIDATE'S DECLARATION

I, ISHA, Roll No. 2K22/MSCPHY/14, student of M.Sc. Physics, hereby declare that the project Dissertation titled "SYNTHESIS OF GRAPHENE QUANTUM DOTS (GQDs) FROM PADDY STRAW FOR BILIRUBIN DETECTION", which is submitted by me to the Department of Applied Physics, Delhi Technological University, Delhi in partial fulfilment of the requirement for the award of the degree of Master of Science, is original and not copied from any source without proper citation. This work has not previously formed on the basis for the award of any Degree, Diploma, Associate ship, Fellowship or other similar title or recognition.

- Paper published in Scopus indexed journal with following details:

  Title of Paper: "Synthesis of graphene quantum dots (GQDs) from Paddy straw for Bilirubin detection".

  Authors Names (In sequence as per Research Paper): Isha, Aneesha, Mohan Singh Mehata

  Name of the Journal: Plasmonics

  Status of Paper: Accepted

  Date of Communication: 08 May 2024

  Date of Acceptance: 06 June 2024

  Published Online: NA

Place: Delhi

Isha

Date: 7 June 2024 **ISHA**

Dr. Mohan Singh Mehata
Former JSPS (Japan) and CAS (China) Fellow

Assistant Professor

Department of Applied Physics
Delhi Technological University
Bawana Road, Delhi – 110042
INDIA
Mob: +91 9953142553
Email: msmehata@dtu.ac.in
msmehata@gmail.com

SUPERVISOR CERTIFICATE

I, hereby certify that the Project Dissertation titled "Synthesis of Graphene Quantum Dots (GQDs) from Paddy Straw for bilirubin detection" which is submitted by Isha, Roll No. 2K22/MSCPHY/14 to the Department of Applied Physics, Delhi Technological University, Delhi in partial fulfillment of the requirement for the award of the degree of Master of Science, is a record of the project work carried out by the student under my supervision. To the best of my knowledge, this work has not been submitted in part of full for any Degree or Diploma to this University or elsewhere.

7/6/2024

Place: Delhi

DR. MOHAN SINGH MEHATA

Date: 07 June 2024

SUPERVISOR

ACKNOWLEDGEMENT

I would like to express my indebtedness and deepest sense of regard to my supervisor, Dr. Mohan Singh Mehata, Assistant Professor, Department of Applied Physics, Delhi Technological University for providing his incessant expertise, inspiration, encouragement, suggestions and his opportunity to work under his guidance. I am grateful for the constant help provided at every step of this project by Ms. Aneesha and all the lab members of Laser Spectroscopy Laboratory, Department of Applied Physics, Delhi Technological University. I am also thankful to my family and colleagues for their invaluable support, care and patience during this project. Lastly, I would thank Delhi Technological University for providing such a wonderful opportunity of working on this project.

ABSTRACT

This work reports the synthesis of blue-emitting graphene quantum dots (GQDs) with an average diameter of 3.8 ± 0.5 nm from paddy straw, a sustainable biomass resource, via hydrothermal synthesis. These GQDs demonstrate excellent performance in bilirubin (BR) detection. The GQD photoluminescence (PL) intensity exhibits a proportional decrease with increasing BR concentration, indicating efficient quenching. The limit of detection for BR reaches a low value of 87.9 nM, highlighting the high sensitivity and selectivity of the GQD-based sensor. The observed quenching likely arises from a combined mechanism involving static quenching due to GQD-BR complex formation, inner filter effect (IFE) and Förster resonance energy transfer facilitated by spectral overlap.

CONTENTS

LIST OF FIGURES

LIST OF SYMBOLS AND ABBREVIATIONS

GQDs	Graphene Quantum Dots
BR	Bilirubin
PL	Photoluminescence
RBCs	Red Blood Cells
AI	7-Azaindole
EDTA	Ethylenediamine-tetra acetic acids
BSA	Bis-(trimethylsilyl)acetamide
DI	Deionized
HCL	Hydrochloric acid
PMT	Photomultiplier tube
NaOH	Sodium hydroxide
XRD	X-ray diffraction
UV-VIS	Ultraviolet – Visible
FTIR	Fourier Transform Infrared
HRTEM	High Resolution Transmission Electron Microscopy
IFE	Inner Filter Effect
FRET	Förster resonance energy transfer
BH plot	Benesi Hildebrand Plot
SV plot	Stern-Volmer Plot
LOD	Limit of Detection

CHAPTER 1

INTRODUCTION

1.1 THE BACKGROUND OF GRAPHENE

Carbon is one of the most abundant elements on earth which plays an important role in the development of advanced and environment friendly materials among other elegant functional materials. Carbon nanostructures have collected all important attention repaid to their striking mechanical vigorous, electrically conductive abilities, and noteworthy chemical and thermal qualities [1]. Along with these properties, Graphene is the strongest and thinnest material due to its distinct 2D honeycomb lattice structure. These properties make graphene as a brilliant material for a wide range of applications. In particular, graphene, known as the principal form of carbon graphite, contains only one layer of carbon atoms joined together by coinciding sp^2 hybrid bonds [2]. Graphene is a zero-bandgap material due to its small overlap between valence and conduction bands. In 1947, P. Wallace studied theoretically the properties of graphene. In 2004, Geim and Novoselov worked on graphene and they were awarded the Nobel prize after 6 years.

The zero-bandgap of material, however impedes its applications in LEDs, transistors and photovoltaics, which needs a tunable and measured band gap. Graphene has significant drawbacks such as poor dispersion in solvents and its ability to aggregate. This implies that it has the capability to undergo many transformations, including quantum dots, nanoribbons and etc. Reducing the lateral dimension of 2D graphene into 0D GQDs, could increase its band gap via quantum confinement effects.

In 2023, Bawendi, Louis E. Brus and Alexei I. Ekimov were awarded the Nobel Prize in Chemistry for the discovery of quantum dots.

1.2 EVALUATION OF EXISTING LITERATURE

1.2.1 Graphene Quantum Dots

Unlikely graphene, GQDs are non-zero band gap materials [3] that exhibit their strong quantum confinement [4] and edge effects [5], for this reason, GQDs possess remarkable optical and electrical properties. They serve important properties such as strong water solubility, low cost, stable photoluminescence (PL), tunable bandgap, good compatibility and low toxicity [6-8]. GQDs possess their unique inner structure and surface chemical groups [9]. GQDs normally have features that drop below a diameter of 20 nm [10]. Because of its small size, GQDs carry a declaration for biomedical applications in comparison with graphene or graphene oxide (GO) [11,12]. The PL can be readily monitored by simply altering the dimension and surface chemistry of GQDs. GQDs originated from paddy straw that can be dispersed in water with strong PL and excellent biocompatibility, presenting better capability for use in biological and medical fields [13]. GQDs have a greater surface area, small size and higher crystallinity. These attractive properties of GQDs make them more desirable for a wide range of applications such as bioimaging [14,15], drug/gene delivery [16,17], anticancer agents [18,19], biosensing [20,21], electronic displays [22] and photocatalysis [23].

1.2.2 Synthesis Routes

GQDs synthesis techniques are often divided into two distinct categories: top-down and bottom-up methods. Bottom-up techniques utilize detailed effective steps and particulate organic elements, imposing obstacles for optimizing circumstances [11]. On the other hand, top-down techniques include breaking down and separating easily available bulk graphene-based materials, like graphite, under the worst circumstances. These procedures typically consist of different steps involving strong oxidizing agents, concentrated acids and elevated temperatures [10]. Top-down techniques include sol-gel method [24], hydrothermal method [25], electrochemical exfoliation [26], chemical oxidation [27], nanolithography [28], microwave-assisted [29] and ultrasonic shearing [13]. Possibly, the large-scale production of high-quality graphene quantum dots (GQDs) from different carbon sources could be achieved by developing a novel methodology that combines that combines the benefits of both top-down and bottom-up techniques. The hydrothermal synthesis technique is a versatile method used to create a wide range of materials, offers advantages such as inexpensive, less reaction time, a safer and feasible experimental plan. The ongoing analysis proves a hydrothermal method for synthesizing GQDs. The precursor is dissolved in a solvent inside the reaction vessel to create a homogeneous solution. The vessel is sealed to create a high temperature and pressure environment is necessary for hydrothermal synthesis. There should be a control of pH and temperature, pH adjustments are made by using acids and bases.

1.2.3 Eco-Friendly Synthesis of GQDs

Biomass waste, described from its green, affordable, abundant, easily accessible, and carbon-rich nature, introduces a promising option as a precursor for creating GQDs. The management and renewal of biomass waste presents an important confrontation in today's world. Effective use of biomass waste not only helps in reusable obstacles but also gives a low- budget source for GQD synthesis. This plan considered using biomass waste as a low-budget and sustainable precursor [30]. Various types of, including plant leaves, paddy straw, coffee grounds, grass and wood charcoal have been used to produce GQDs with product yield almost equivalent to graphene-based extravagant precursors. There are many methods for the synthesis of quantum dots from biomass wastes such as agriculture wastes, industrial wastes, urban wastes, livestock wastes and forestry wastes as shown in Fig 1.1. Agriculture waste-based quantum dots have a wide range of applications due to their excellent optical, thermal, mechanical and electrical properties. The predominant sources of agricultural biomass include sugarcane bagasse, corn straw, rice residue and wheat stem. Several synthesis methods have been used to produce carbon-based nanomaterials from biomass waste. However, green synthesis strategies that involve energy saving approaches are gaining more attention.

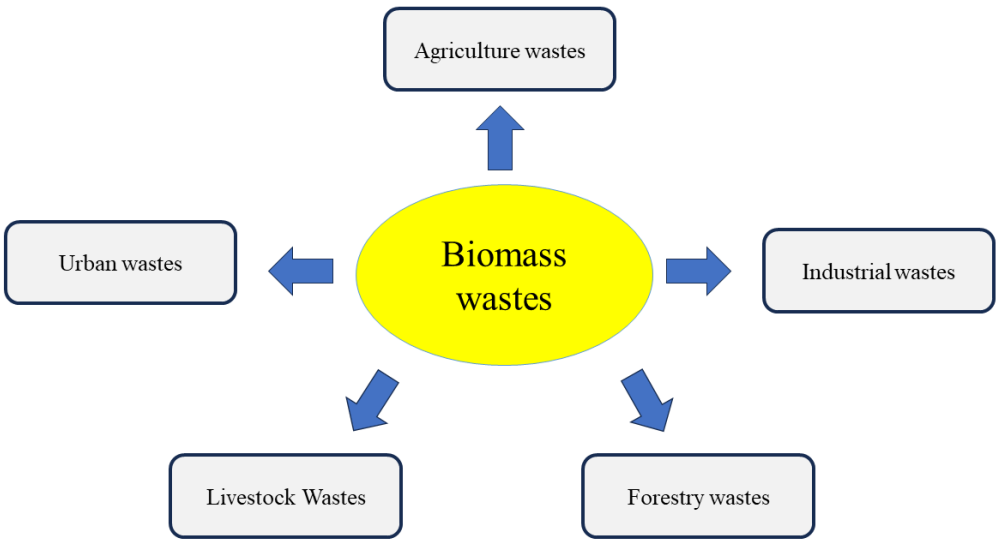

Figure 1.1 Major Sources of Biomass wastes

1.3 Paddy Straw

Rice is one of the highest-expanded crops globally [31] however, agricultural waste for example, paddy straw is a usual agricultural residue that consists of generous carbon content because of the existence of cellulose and lignin [32]. The maximum paddy straw manufactured is currently inclined through open field burning. This procedure leads to air pollution, energy wastage, and the occupation of landfill areas [33]. Constructively modifying paddy straw biomass waste into valuable products can capitulate essential economic and environmental benefits [34]. Paddy straw also contains a large amount of silica which can help to prepare silica-based materials, silica [35], silicon [36], silicon nitride [37] and zeolites [38].

1.4. BILIRUBIN (BR)

Bilirubin (BR) is a yellow pigment with a structural formula, as shown in Fig 1.2., produced during the instinctive breakdown of red blood cells (RBCs) as part of the body's cleansing process [39]. It is an important component of bile, an essential digestive liquid the liver produces. There are three distinct forms of bilirubin: free bilirubin, direct bilirubin and total bilirubin. The typical concentration of free bilirubin in the bloodstream of humans is approximately 25μM. Beyond this threshold, bilirubin becomes harmful to human cells. Increased bilirubin levels in the bloodstream can cause jaundice, which is marked by yellowing of the skin and eyes. Under normal physiological conditions, bilirubin undergoes direct conjugation (which means conjugation with glucuronic acid) in the liver, resulting in the formation of a water-soluble complex. This complex is then eliminated in both bile and urine. The unconjugated bilirubin is recognized as potentially harmful. Uplifted steps of unconjugated BR in the blood are important signs of many strict situations such as jaundice, hyperbilirubinemia, etc. [26,27]. Newborn babies frequently experience hyperbilirubinemia as a result of an excessive amount of bilirubin in their bloodstream. This condition results in the discoloration of the baby's skin, eyes and other tissues. Various experimental techniques have been developed to detect BR, including enzymatic test [42], polarography [43], high performance liquid chromatography (HPLC) [44], piezoelectricity [45], chemiluminescence [46] , electrochemical methods [47] and Raman spectroscopy [48]. Nevertheless, the above mention approaches have several limitations, including intricate instrumentations, inadequate selectivity, and reduced sensitivity. Fluorometric detection of biomolecules is extremely desirable due to its simplicity, quick reaction, high selectivity, enhanced

sensitivity across a wide range of concentrations. The GQDs produced exhibit high and particular sensitivity to BR, making them potentially useful for bilirubin (BR) detection purposes.

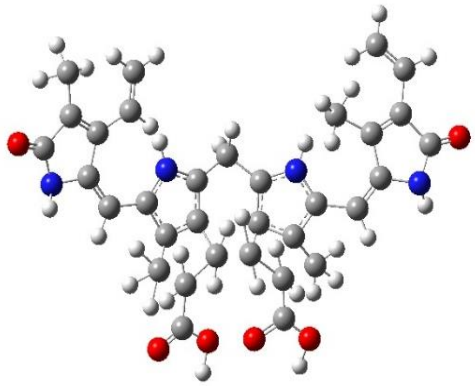

Figure 1.2. Structure of Bilirubin

AIM AND SCOPE OF STUDY

I. Synthesis of Graphene Quantum Dots from Biomass waste, Paddy straw.

II. Analyzing the crystal structure, morphology and stability of the biosynthesized GQDs using various characterization techniques.

III. Investigating the interaction of GQDs and BR Biomolecules for enhanced stability.

IV. Examine the FRET mechanism between GQDs and BR.

CHAPTER 2

EXPERIMENTAL SECTION

2.1. MATERIALS

The agricultural waste of paddy straw was gathered from Pundri village in the Kaithal district of Haryana, India and kept in dry conditions at room temperature to serve as a precursor for synthesizing GQDs. The analytes bilirubin, urea, uric acid, fructose, glucose, 7-azaindole (AI), ethylenediamine-tetra acetic acid (EDTA), bis-(trimethylsilyl)acetamide (BSA) were all acquired from CDH chemicals. Deionized water (DI) and hydrochloric acid (HCL) are utilized to prepare solutions for the analysis.

2.2. SYNTHESIS OF GQDS

A specimen of paddy straw weighing 2.0 g was taken, washed thoroughly with DI water, dried, and then ground into fine powder using mechanical crushing. Subsequently, the powder was heated at 50^{o} C for 3 h after being washed with 0.15 M HCl. Further, in 25 mL of water, 150 mg of crushed paddy straw was mixed and then placed in an oven for 7 h in a teflon-lined autoclave at 160^{o} C. After cooling, the solution was filtered with a pore size of filter to be 11μM and additionally, the GQDs were further purified by centrifugation at 8,000 rpm for 15 minutes, which separates them from any bigger precursor materials, byproducts, or contaminants that might be penetrated through the filter paper. This byproduct was gathered at the tube's bottom as precipitation in the form of silica. We collected the supernatant and used it for the experiment. Precipitates were thrown away. Fig 2.1. depicts a schematic illustration of the GQDs preparation procedure.

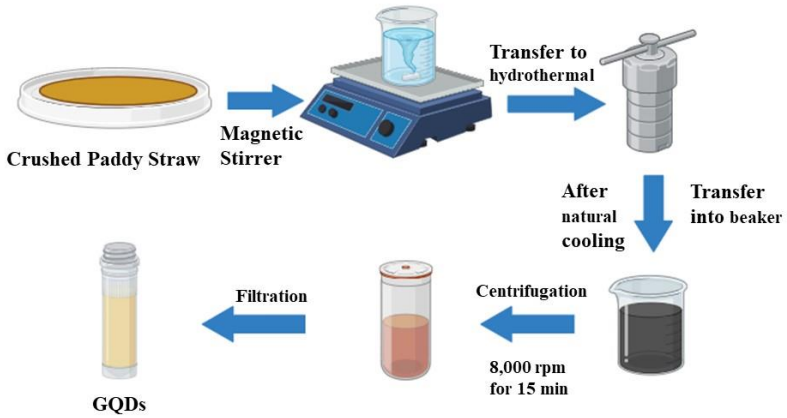

Figure 2.1. Schematic preparation of GQDs from Paddy staw

2.3. PREPARATION OF BILIRUBIN SOLUTION

A stock solution of bilirubin (1mM) was prepared by dissolving the required quantity of bilirubin in water by adjusting the pH to 8 using a 1M NaOH solution, as bilirubin does not dissolve in water, but it becomes soluble in an alkaline environment. A small portion was then taken from this stock solution, and the pH was adjusted accordingly for the experimental requirements using a 1 M HCl solution when needed. All experiments were conducted in low-light conditions.

CHAPTER 3

CHARACTERIZATION TECHNIQUES

UV – vis spectroscopy experiments were used to analyse and study absorption spectra using a dual–beam UV/vis spectrometer (Lambda 750, Perkin Elmer, USA) (Fig 3.1.) [49]. For the samples, a quartz cuvette with optical path of 10 mm was used. The Fluorolog-3 spectrofluorometer (Horiba Jobin Yvon) (Fig 3.2.) was utilized to record PL and PL-excitation measurements which was configured with a photomultiplier tube (PMT), 450W xenon, and flash lamps. Using Bruker D8 advance (Fig 3.3.) which is equipped with a Cu (K_α) radiation source with an accelerating voltage of 40kV and 20mA current, X-ray diffraction (XRD) patterns were obtained [1].

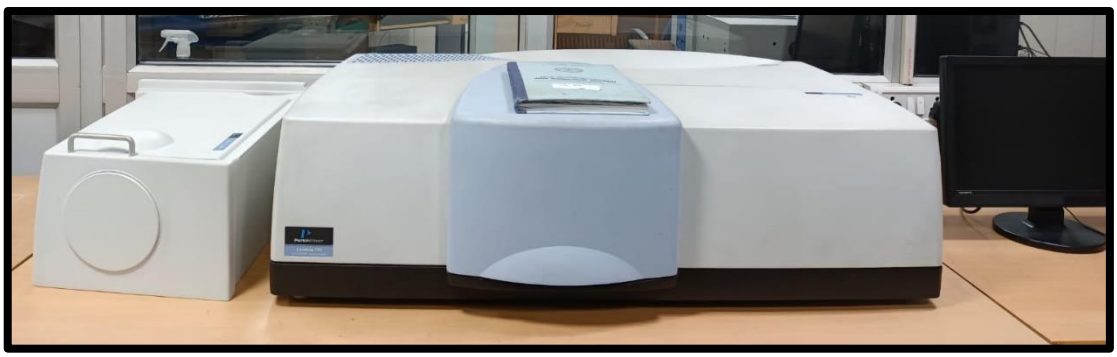

Figure 3.1. Perkin Elmer Lambda 750 UV/Vis/NIR spectrophotometer

Figure 3.2. Horiba Jobin Yvon Fluorolog-3 spectrofluorometer

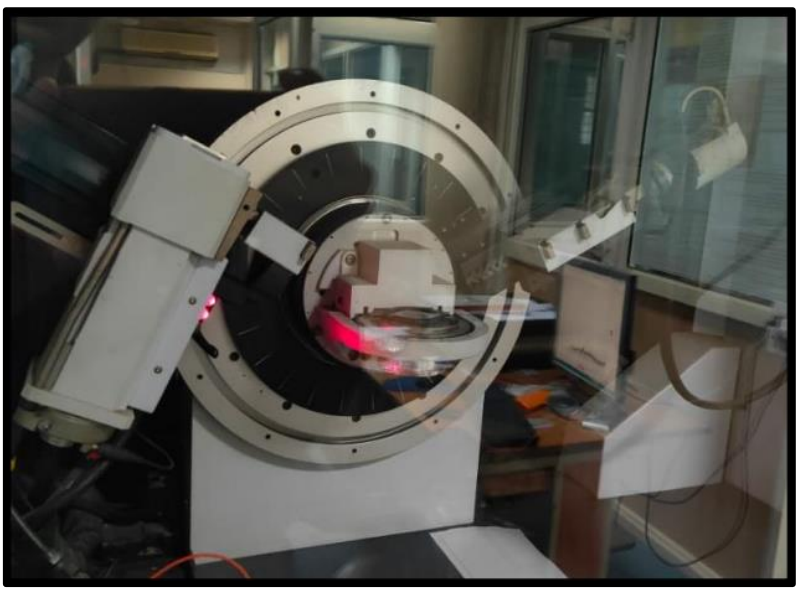

Figure 3.3. Bruker's D-8 Advanced X-Ray Diffractometer

High-resolution images of the GQDs were taken by transmission electron microscopy (TEM) with an accelerating voltage of 200 kV using TALOS thermos-scientific instruments (Fig 3.4.). Fourier-transform infrared spectroscopy (FT-IR) (Fig 3.5.) was used to obtain the spectra under the frequency range 500-4000 cm^{-1} range using Perkin Elmer, FTIR spectrometers.

Figure 3.4. TALOS thermos-scientific instrument

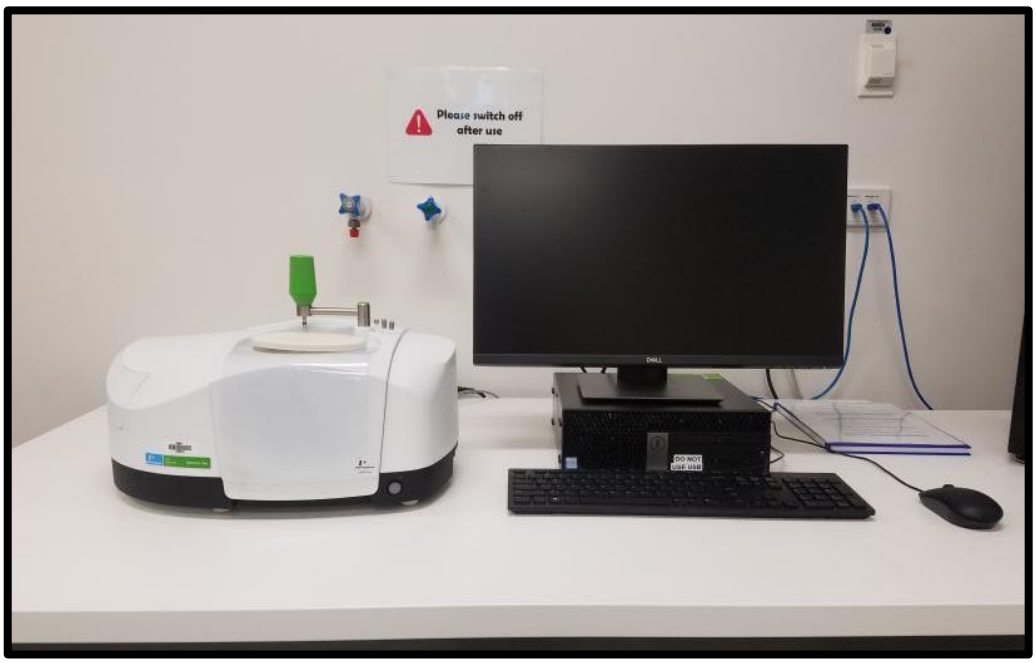

Figure 3.5. Perkin Elmer Two-Spectrum FTIR spectrometers

CHAPTER 4
RESULT AND DISCUSSION

4.1. X-RAY DIFFRACTION

The XRD was utilized to study the structural property. Fig 4.1. displays the peak at 25.4^{o}, which corresponds to the (002) diffraction plane in the XRD of GQDs [1,29]. The highest peak in the figure may indicate the existence of residual silica ions [30,31]. This silica may come from the sediment remaining at the bottom of the centrifuge [53].

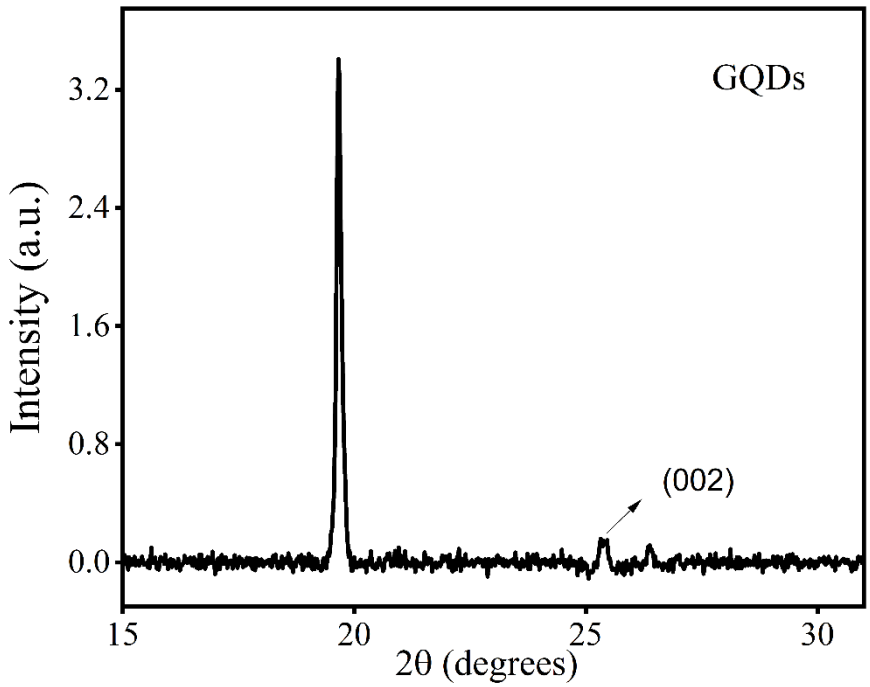

Figure 4.1. XRD pattern of GQDs.

4.2. HRTEM ANALYSIS

The fabricated GQDs were also analyzed through TEM, as illustrated in Fig 4.2.(a). To prepare the sample, drop the sample solution onto a grid of copper and then allow it to dry at room temperature. The size distribution of the GQDs, which is 3.8 ± 0.5 nm is illustrated in Fig 4.2.(b). The observed spherical particles are fairly polydispersed.

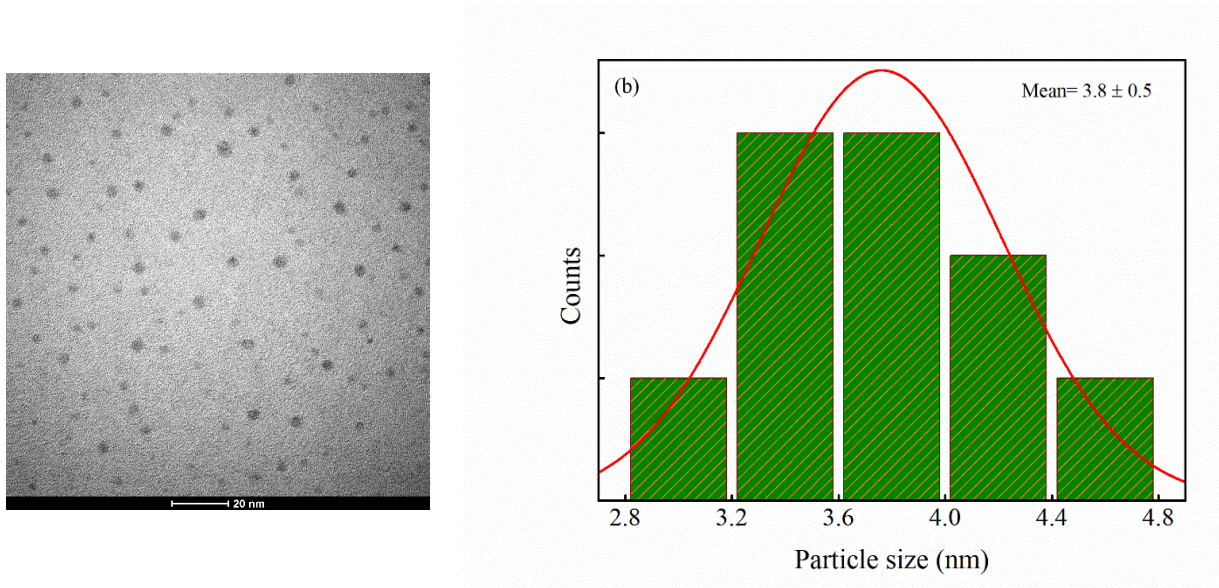

Figure 4.2 TEM images (a) and size distribution (b) of GQDs.

4.3 FTIR ANALYSIS

Fig 4.3. depicts the FTIR spectra of GQDs, where a wide band at 3318 cm^{-1} is assigned to the stretching vibrations of amine (N-H) and hydroxyl (-OH) groups [54]. The presence of OH and C-H linkages is revealed by the peak observed at 2112 cm^{-1}. The stretching vibrations of C-O and aromatic rings C=C, which correspond to epoxy and ether groups, respectively are responsible for the observed peaks at 1639 and 1103 cm^{-}

[1] [55]. Because of the abundance of oxygen-bearing functional groups, GQDs are allowed to remain stably suspended and effortlessly disperse in water.

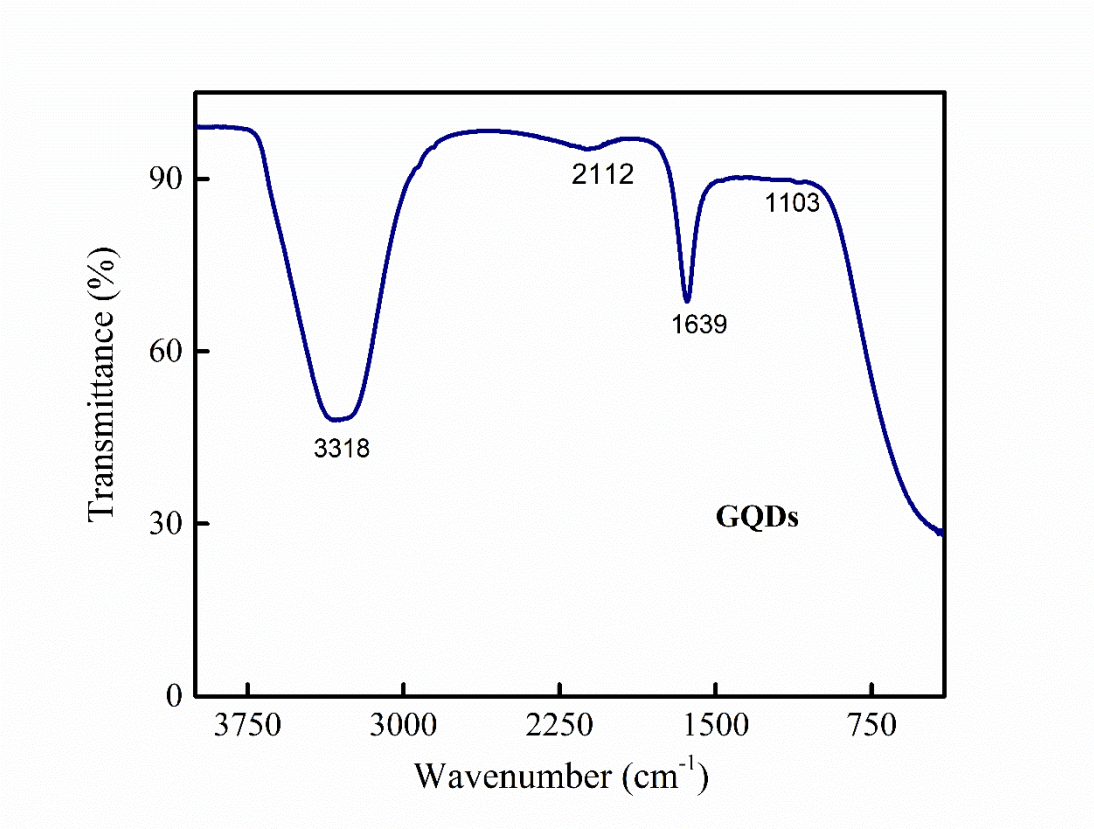

Figure 4.3. FT-IR spectrum of GQDs.

4.4. UV-VIS ABSORPTION SPECTRA

The optical parameters of GQDs were examined using a steady-state spectroscopic technique. The UV-vis absorption spectrum of GQDs is illustrated in Fig 4.4., showing a prominent absorption peak in the UV region at around 278 nm. The intense and sharp peak of absorption below 300 nm exhibits the π-π* transitions of the C=C aromatic bonds, indicating the involvement of sp^2 hybridization domains. Also, the functionalized oxygen group on the surface of GQDs generates an absorption associated with the n-π* transition of the C=O bonds, which is observable in the region

of 290-320 nm [49]. Upon stimulation at the excitation wavelength, the GQDs demonstrate intense PL.

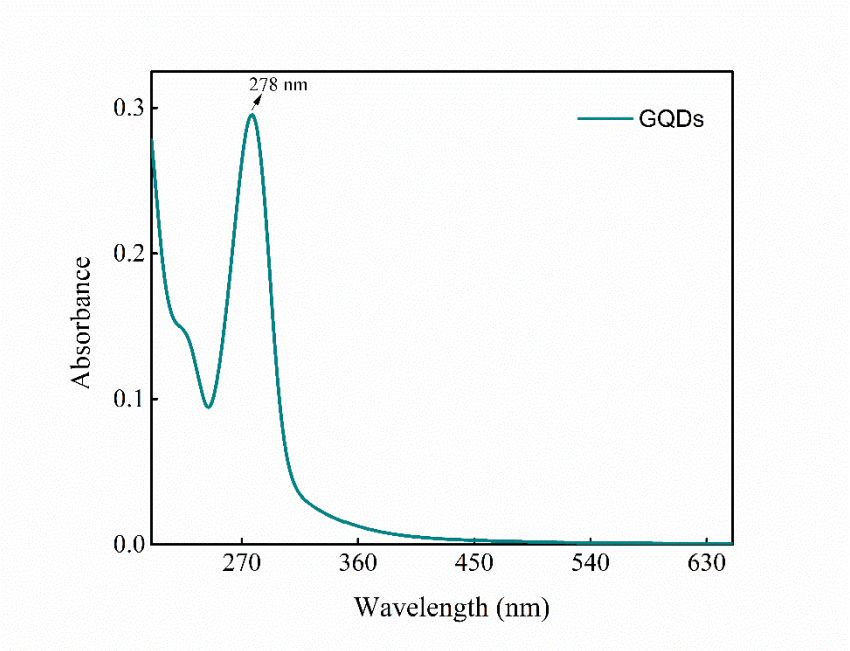

Figure 4.4 UV-vis spectrum of GQDs.

From the absorption spectra, the optical bandgap of the GQDs was determined by using a Tauc plot [56], which illustrates the relationship between $(\alpha h\nu)^{1/\gamma}$ *vs.* photon energy hν. The γ factor, which is reliant upon the nature of the material, is ½ for direct and 2 and indirect bandgap materials respectively [57]. Therefore, a direct bandgap of GQDs was estimated to be ~ 4.07 eV as illustrated in Fig 4.5.

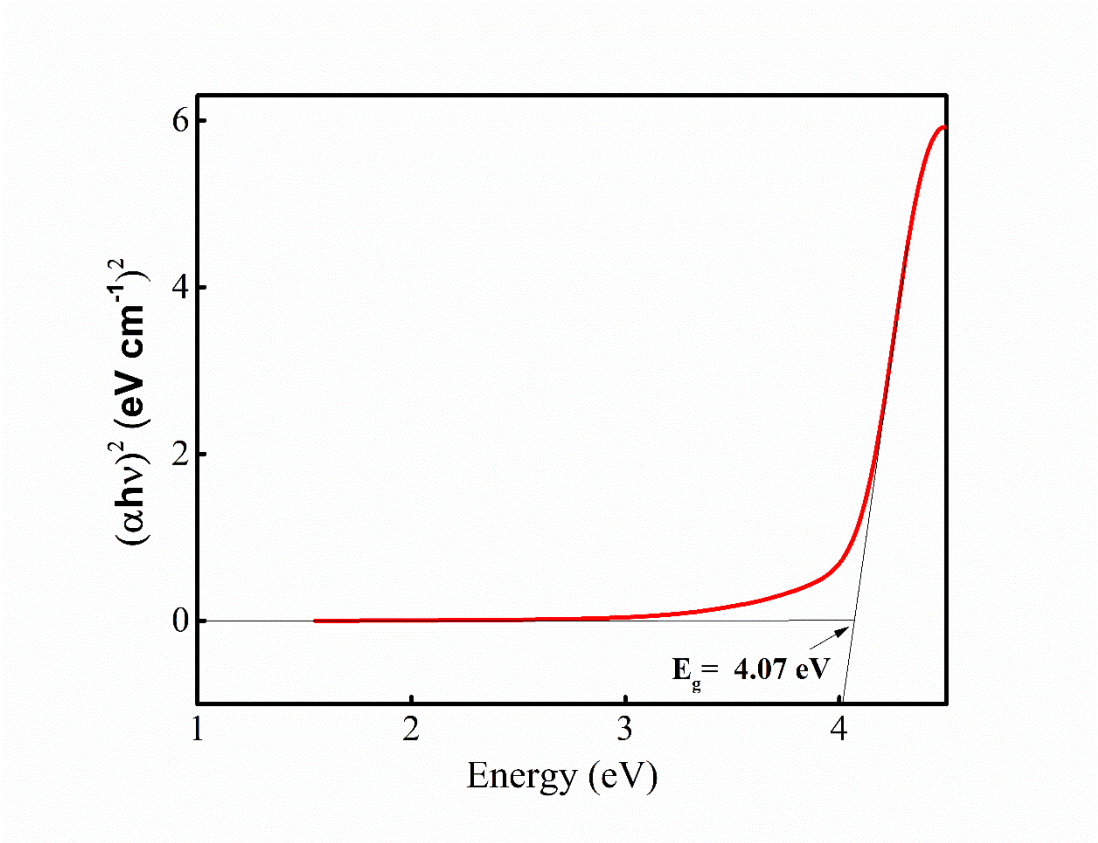

Figure 4.5 Tauc plot for direct band gap of GQDs.

4.5. PHOTOLUMINESCENCE SPECTRA

The optical properties were further investigated, and photoluminescence (PL) spectra were studied across a wide range of excitation wavelengths. As illustrated in Fig 4.6. (a), when excited at a wavelength of 370 nm, the PL spectra exhibit a broad peak with maximum intensity at 450 nm and the position of the peak changes gradually with variations in excitation wavelengths Fig 4.6.(b). A large stokes shift is observed with excitation wavelength [58]. The intensity of PL from the GQDs decreases as the excitation wavelength increases, resulting in a redshift. PL maximum shifted in response to variations in the excitation wavelength. The Stokes shift in wavelength offers a beneficial feature for utilizing GQDs in sensing applications [38-40]. Using

quinine sulphate, which has a quantum yield (QY) of 54% as a reference, it was determined that the QY of GQDs was 3.5 % using the equation.

$$QY_{sam} = QY_{ref} \left(\frac{PL_{sam}}{PL_{ref}} \right) \left(\frac{Abs_{ref}}{Abs_{sam}} \right) \left(\frac{\eta_{sam}}{\eta_{ref}} \right)^2$$

where QY_{ref} indicates the quantum yield of quinine sulphate and QY_{sam} indicates quantum yield of GQDs. Abs indicates the absorbance of reference and GQDs, and the integrated areas of PL spectra are represented by PL_{sam} and PL_{ref} and η represent the refractive index of distilled water and sulfuric acid which are used as the solvents in QDs and reference respectively.

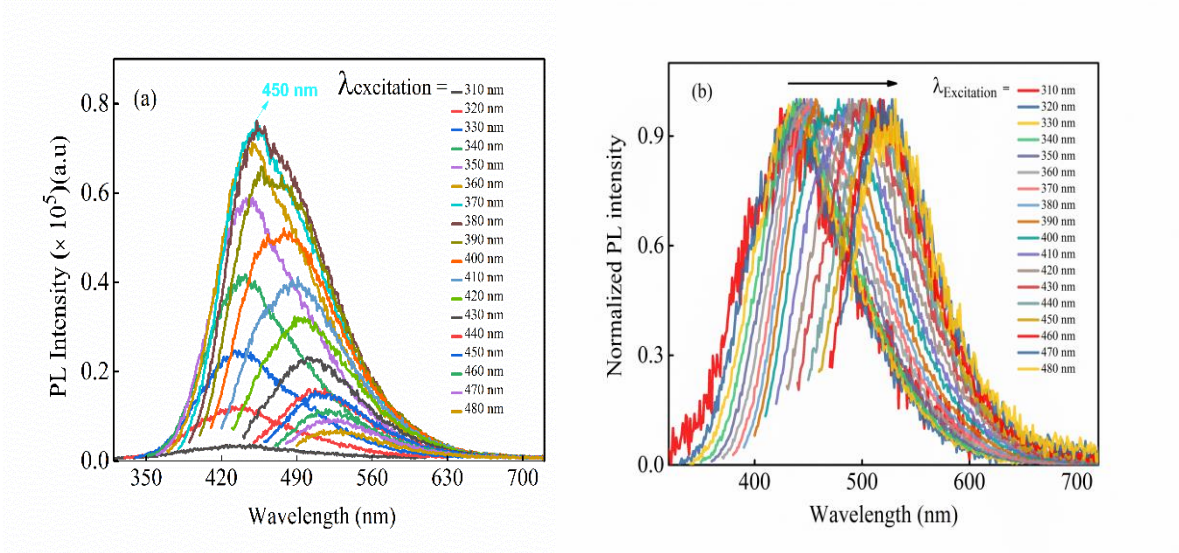

Figure 4.6. Photoluminescence spectra at a range of excitation from 310-480 nm (a) and normalized PL spectra (b) of GQDs.

4.6. INTERACTION WITH BR

Upon adding the different concentration of bilirubin in GQDs, there involves interaction between GQDs and bilirubin as shown in Fig 4.7. that leads to the formation of a stable complex due to bonding between the hydroxyl group of BR and functional groups of the GQDs in the ground state.

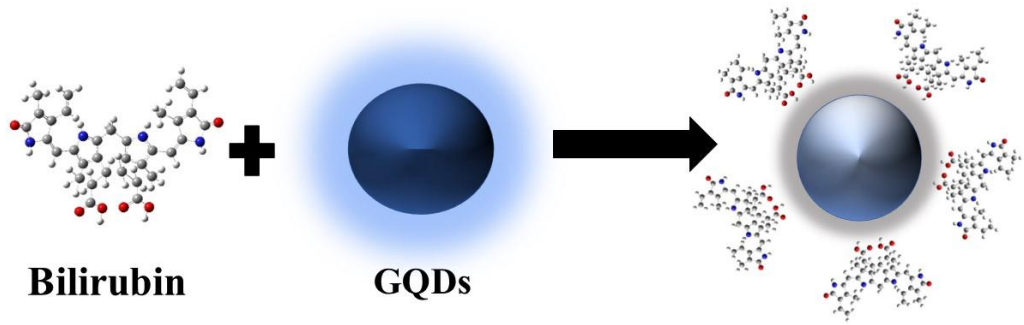

Figure 4.7. Complex formation by interaction of GQDs with BR.

4.6.1 Absorption of BR

Various concentrations of bilirubin were prepared in an ideal environment to analyze the sensing capabilities of GQDs. As illustrated in Fig 4.8., the absorption spectra of GQDs at different concentrations ranging from 9.9 μM to 115 μM were observed, with and without the presence of BR. Along with the absorption intensity at 278 nm, the band-edge absorption intensity at ~ 327 nm also increased. The intensity of the band-edge increased due to the n-π* transition in GQDs. When the concentration of BR increases, the intensity of the absorption also increases and is nearly constant at the concentration of 115 μM and higher [62]. The increase in the absorption intensity indicates the interaction between GQDs and BR. This interaction might involve the formation of a stable complex due to bonding between the hydroxyl group of BR and functional groups of the GQDs in the ground state. Such complex formation between GQDs and BR potentially leads to enhanced absorption intensity at 278 nm without showing any extra peak of BR. To further strengthen the evidence for this interaction, the Benesi-Hildebrand (BH) method was employed [8]. The plot of $1/(A_0\text{-}A)$ *vs.* 1/conc. of BR, where A_0 represents the absorbance without BR and A represents the

absorbance with BR in the range of 0-115 µM is quite linear with $R^2 = 0.99$, as depicted in the inset of Fig 4.9. The plot indicates the formation of a 1:1 complex between BR and GQDs. The calculated binding constant (K_b) is 5.15×10^3 M^{-1} [63]. The linear relation observed between the absorbance of GQDs and the concentration of BR signifies that GQDs can be utilized as a probe for the detection of BR.

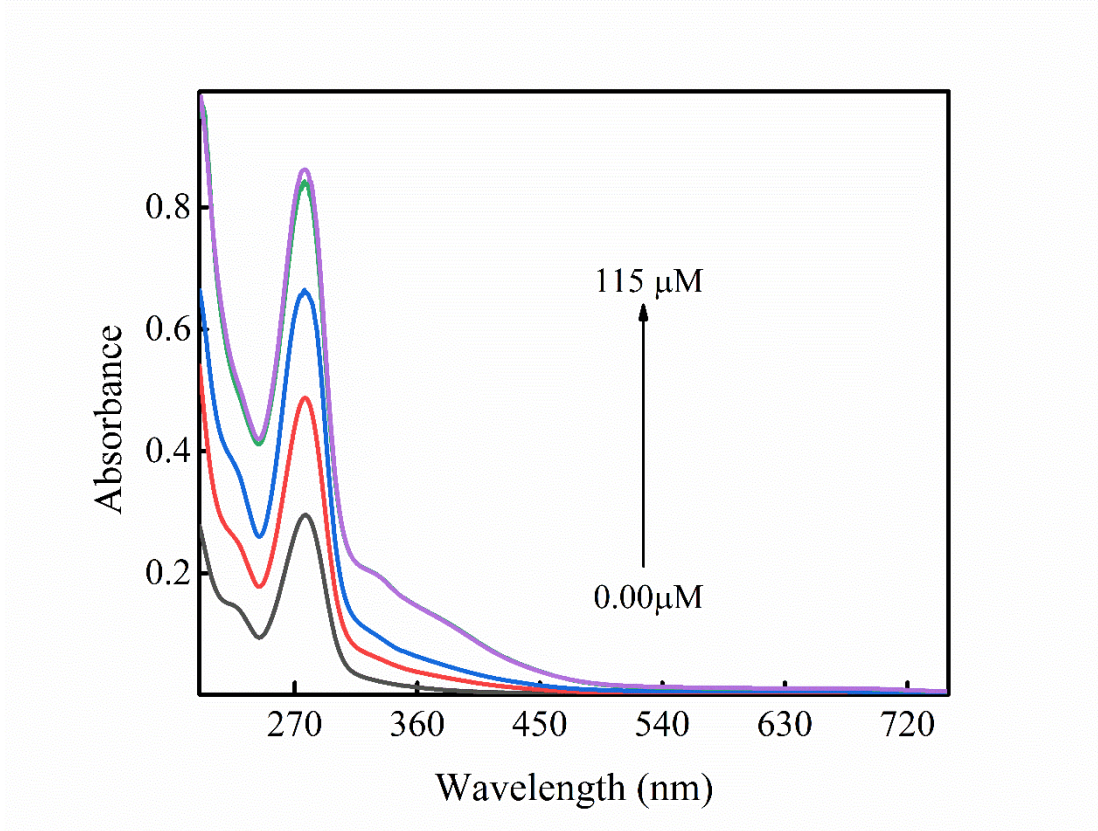

Figure 4.8. Absorbance spectra of GQDs in the absence and presence of multiple BR concentrations.

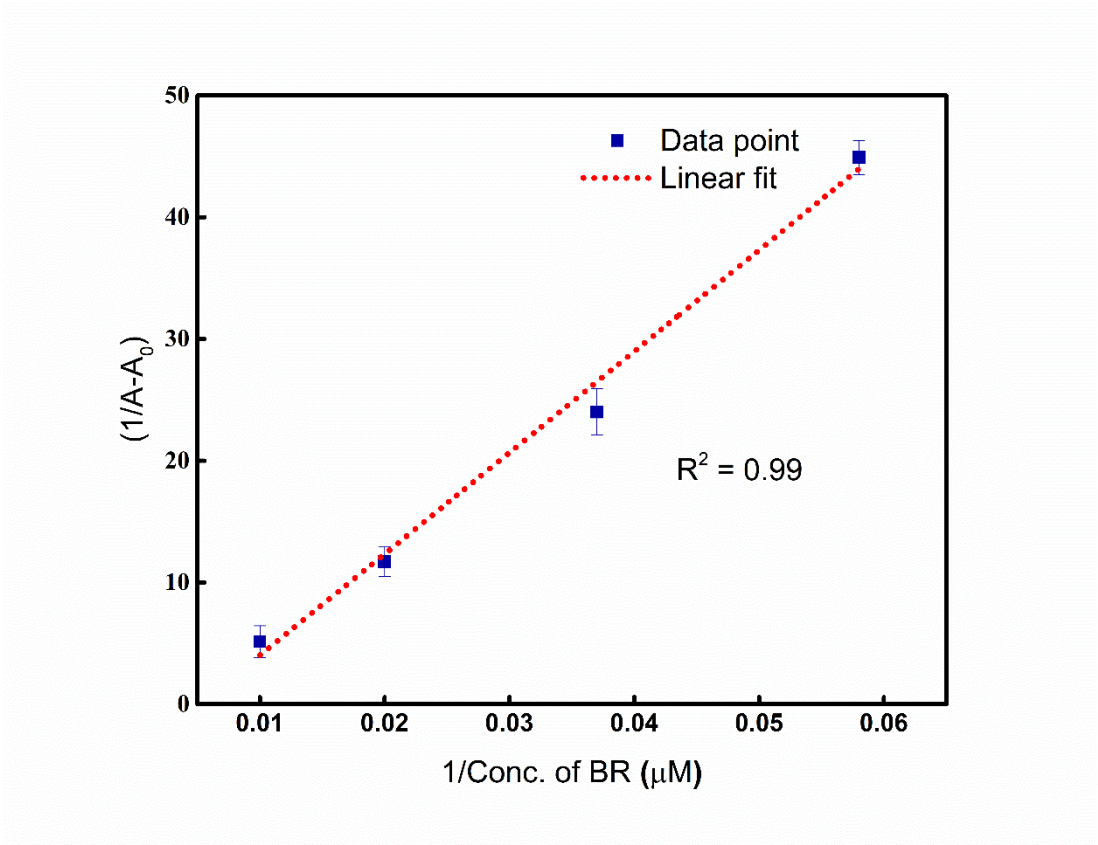

Figure 4.9. Plot (B-H) of $(\frac{1}{A-A0})$ vs [1/Q]

4.6.2 Fluorescence of BR

Before bilirubin addition, the PL spectra exhibited a peak at 450 nm when excited with a wavelength of 370 nm. To analyze the PL, different concentrations of bilirubin were mixed with the GQDs solution and it has been acclaimed that if there is an increase in the concentration of bilirubin, the PL intensity of the GQDs was significantly reduced as shown in Fig 4.10. Gradually adding bilirubin aliquots led to a consistent decrease in peak intensity. At a bilirubin concentration of 115 µM, almost 90% of the intensity was quenched. While the findings suggest the formation of a ground-state complex between BR and GQDs, also leads to the quenching of GQDs PL intensity along with several possible mechanisms such as non-fluorescent ground-state complex, inner filter effect (IFE) and Förster resonance energy transfer (FRET) [64]. The reduction in

peak intensity corresponding to a specific bilirubin concentration was quantified using a Stern-Volmer (SV) plot that shows a relationship between the PL intensity ratio (I_0/I)-1 *vs*. bilirubin concentration, where I and I_0 represent the PL peak intensity in the presence and absence of bilirubin respectively. Based on the plot analysis, a linear regression ($R^2 = 0.99$) was obtained within the range of 9.9-115 µM, as depicted in the inset of Fig 4.11. A linear relation indicates possibly a static quenching process involving a single kind of binding site or a possible collisional quenching mechanism. Thus, the linear SV and BH plots support predominantly the static quenching. The calculated value of K_{sv} from the S-V plot was determined to be 7.79×10^3 M^{-1}, suggesting that GQDs have significant potential for detecting bilirubin with high sensitivity. The estimated value of the limit of detection (LOD) was determined to be 87.9 nM.

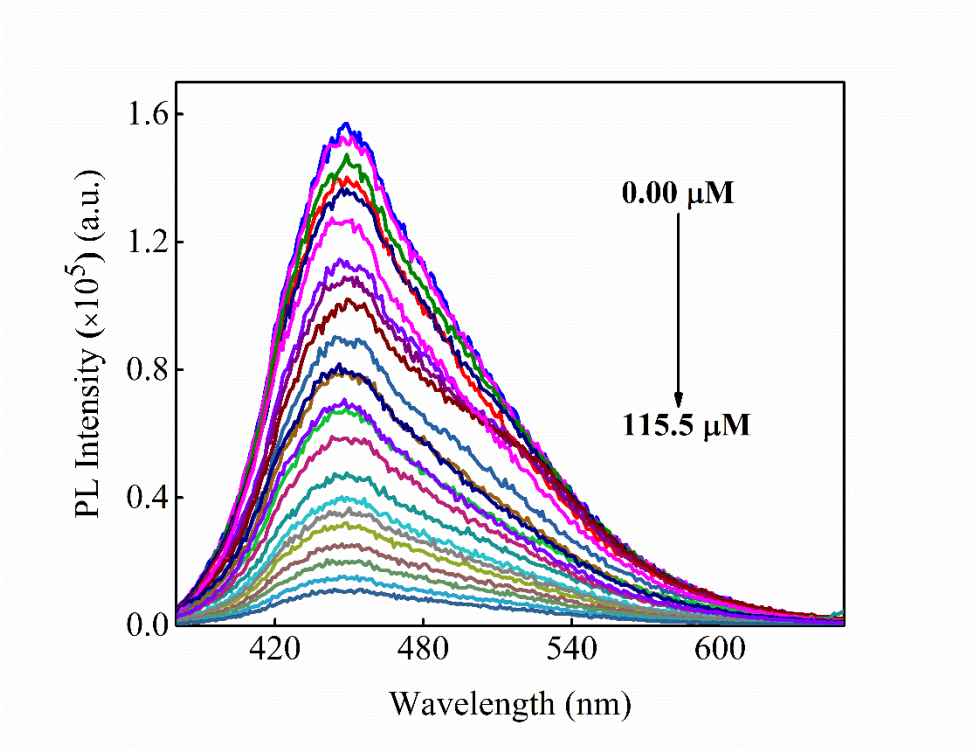

Figure 4.10. Photoluminescence spectra of GQDs in the absence and presence of multiple BR concentrations.

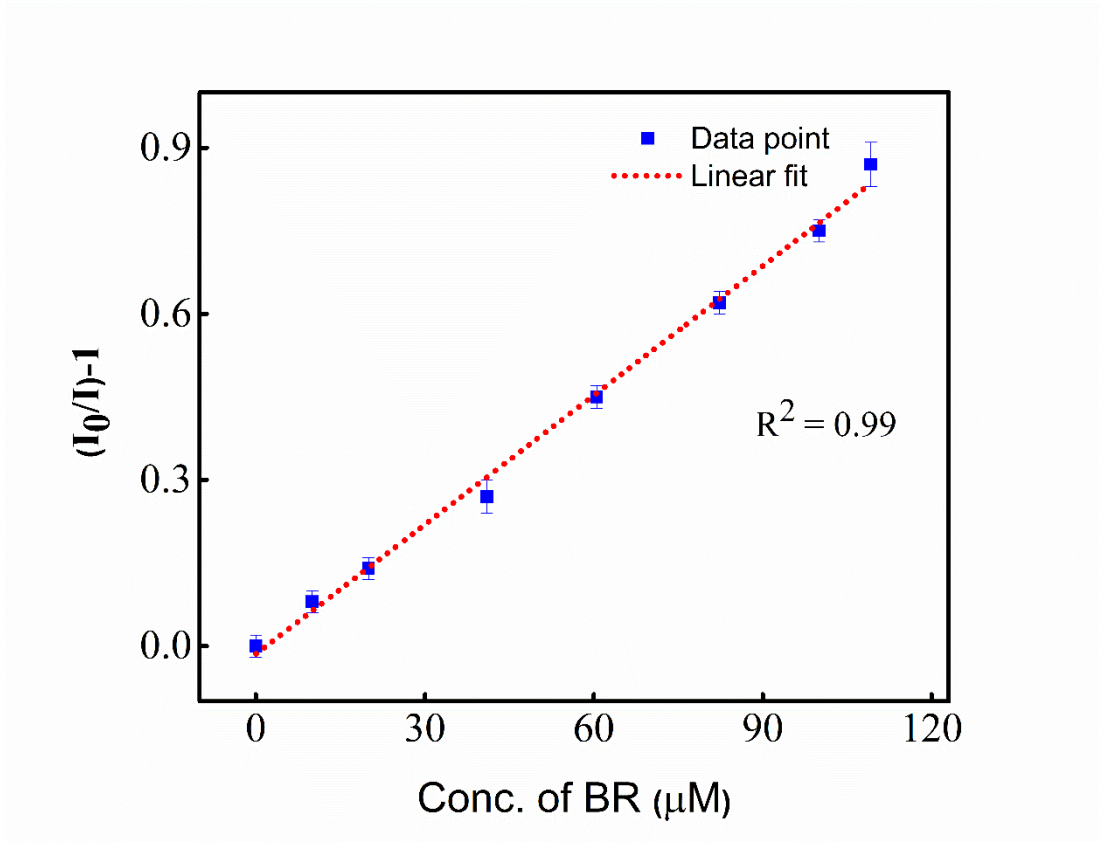

Figure 4.11. S-V plot of $(I_0/I)-1$ vs concentration of BR.

4.6.3 FRET MECHANISM

As shown in Fig 4.12., the spectral overlap between the PL spectrum of GQDs as donor and the absorption spectrum of BR as acceptor indicates the chances of FRET mechanism [65]. As the PL spectrum of GQDs significantly overlaps with the absorption spectrum of BR, there is a possibility of energy transfer from excited GQDs to bilirubin molecules through FRET. The energy transfer would decrease the PL intensity of GQDs. By using an equation $J(\lambda)=\int_{\infty}^{0} F_D(\lambda)\varepsilon_A(\lambda)\lambda^4 d\lambda$, the spectral overlap integral, denoted by J(λ) is determined. The value of J(λ) is calculated to be $9.015 \times 10^{17} nm^4 M^{-1} cm^{-1}$ where $F_D(\lambda)$ and $\varepsilon_A(\lambda)$ represents the donor fluorescence intensity and acceptor's extinction coefficient at λ respectively.

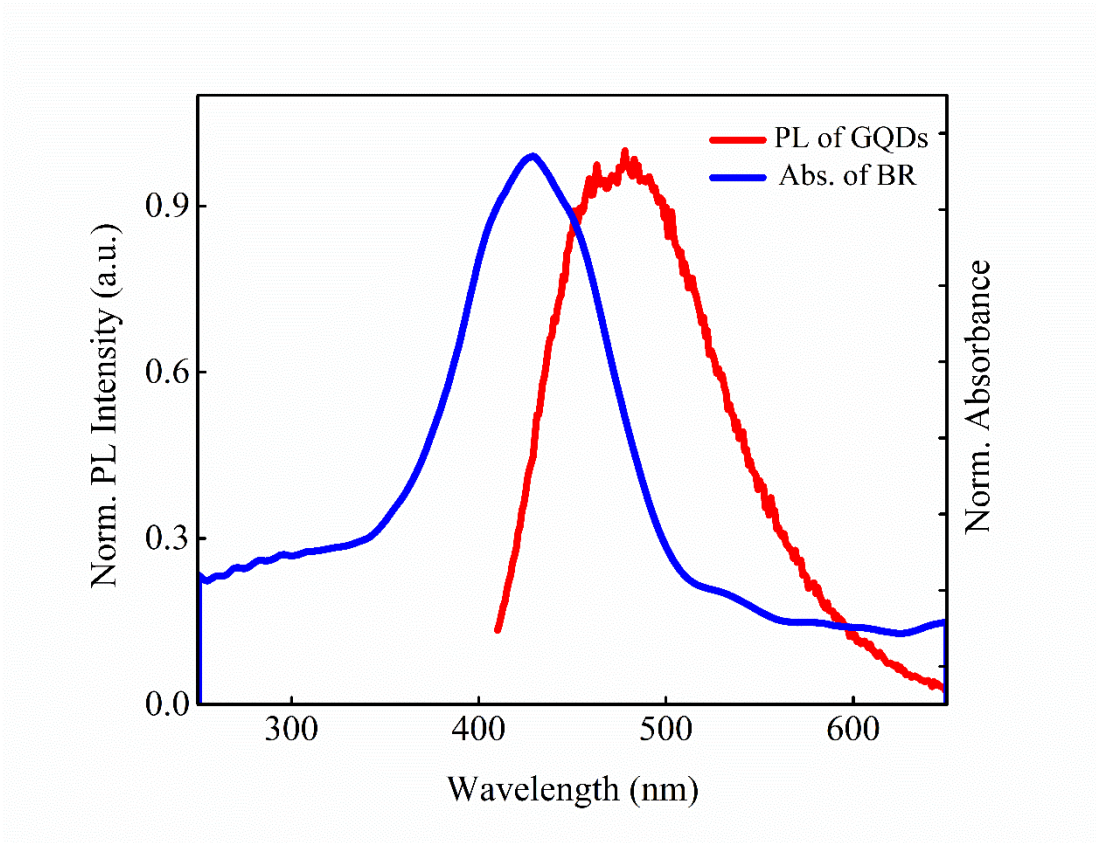

Figure 4.12. Overlapped normalized absorption spectrum of BR and PL spectrum of GQDs.

4.7. SELECTIVITY OF BR

Blue-emitting GQDs could detect bilirubin with the result of some parameters such as strong PL, high sensitivity, and selectivity of GQDs towards bilirubin. GQDs feature hydroxyl (-OH), epoxy and carboxyl groups among other functional groups on their surface. These functional group interacts with the hydroxyl group of bilirubin, potentially leading to the observed quenching of GQDs PL intensity with increasing concentration of BR [65]. The PL-based sensor's ability to selectivity detect bilirubin was assessed by testing it with various biomolecules commonly encountered in biochemical engineering, including urea, uric acid, ascorbic acid, 7AI, glucose, fructose, EDTA and BSA. Then, it was cleared that BR selectively quenched the PL

of GQDs, whereas other biomolecules used for testing were not able to quench, as shown in Fig 4.13. and GQDs absorption intensity increases with the addition of BR but when GQDs interact with other biomolecules given, there is no increase in intensity as shown in Fig 4.14. These biomolecules have the potential to interfere with the specific detection of bilirubin in the biomedical field.

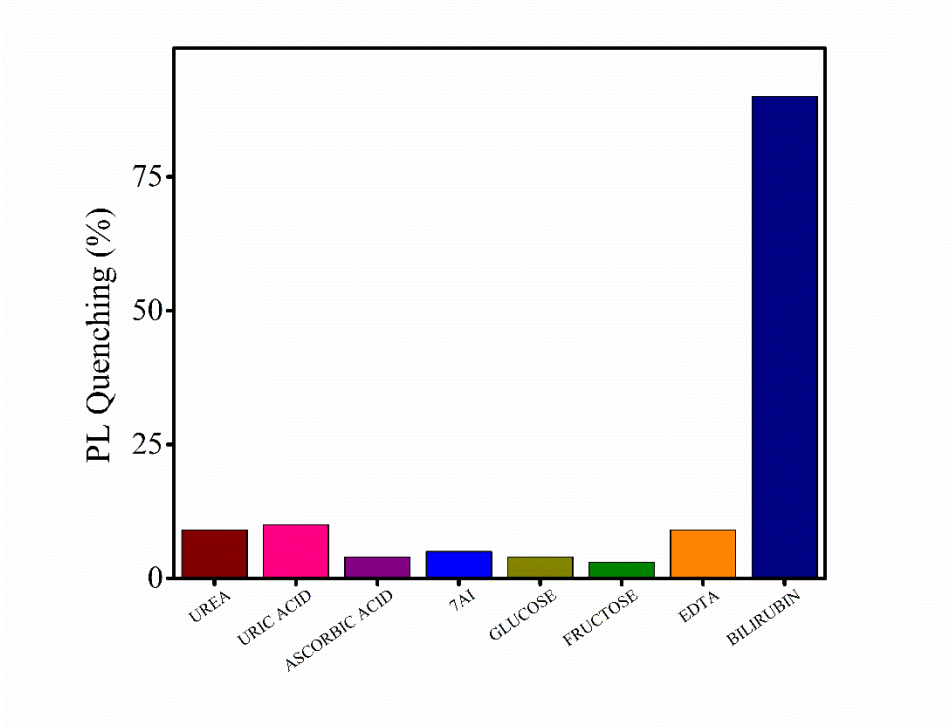

Figure 4.13. Bar diagram of GQDs with BR.

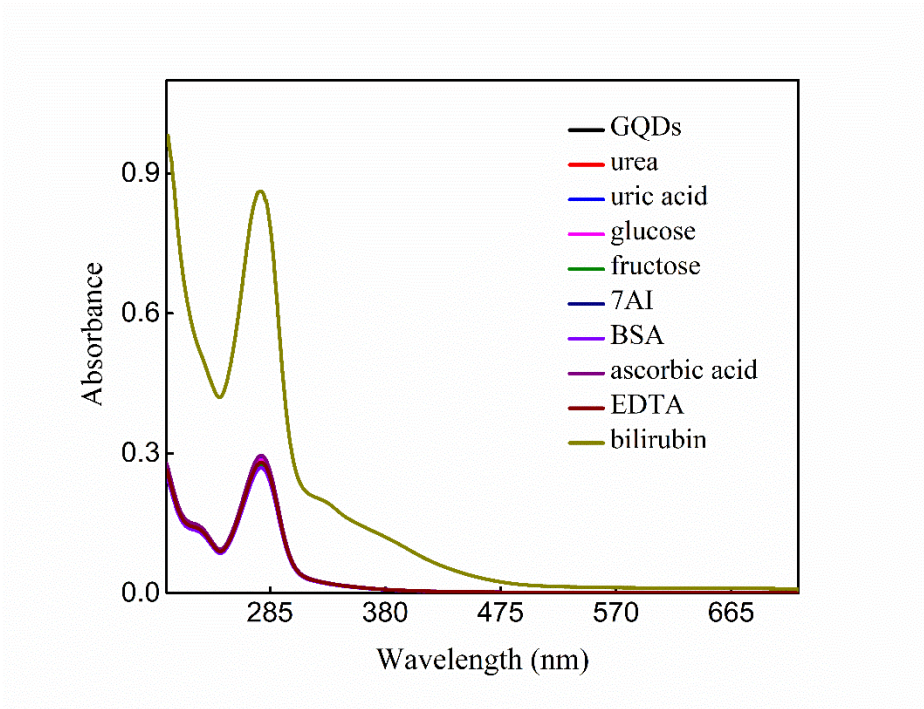

Figure 4.14 Absorption spectra of GQDs with other analytes.

4.8. STABILITY OF GQDs

Fig 4.15. shows the stability of GQDs by comparing the PL intensity as a function of months. The more stable GQDs can be utilized successfully for various biomedical applications. The PL spectra of synthesized GQDs were measured every month from May to February. A slight decrease in the PL intensity was noticed even after 10 months without any shift in the maximum emission wavelength.

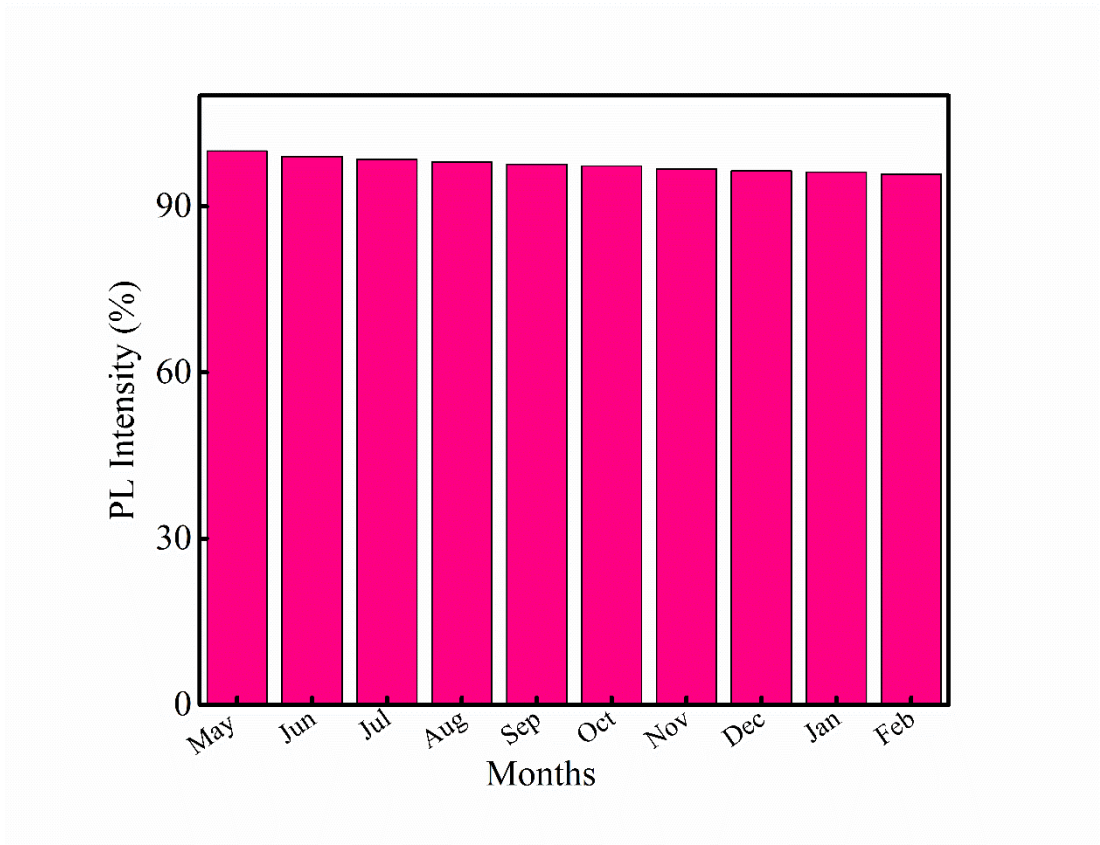

Figure 4.15. PL intensity (%) of GQDs with a period in months, showing stability/photostability of GQDs.

CHAPTER 16

CONCLUSION

Water-dispersible GQDs with an average diameter of 3.8 ± 0.5 nm were developed from paddy straw using a hydrothermal synthesis technique. The GQDs are showing bright blue photoluminescence under 365 nm irradiation and achieve the strongest PL intensity at the 450 nm band with 370 nm excitation. The PL of GQDs was strongly quenched by the presence of bilirubin following the formation of a non-fluorescent ground-state complex (static quenching), inner filter effect (IFE) and Förster resonance energy transfer (FRET) as a quenching mechanism. The GQDs demonstrated high selectivity and sensitivity in detecting bilirubin. The large value of K_{sv}. i.e., 7.79×10^{3} M^{-1} indicates their potential for sensitive bilirubin detection with a limit of detection (LOD) of 87.9 nM. A calibration plot for GQDs PL quenching by bilirubin showed a linear range between 9.9 µM – 115 µM.

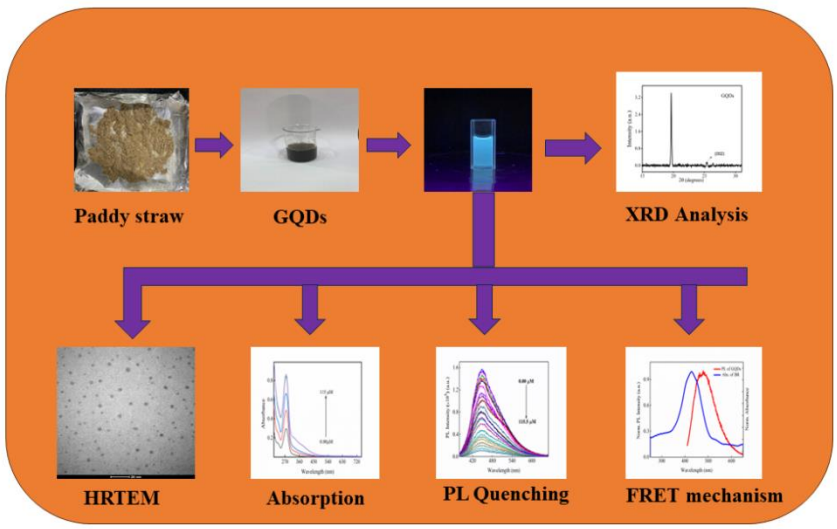

Figure 5.1. Graphical Abstract

REFRENCES

[1] A. Kumar Chaturvedi, A. Pappu, A. Kumar Srivastava, and M. Kumar Gupta, "Synthesis dielectric and mechanical properties of paddy straw derived graphene quantum dots-stone waste nanocomposite," *Mater Lett*, vol. 301, pp. 130323, 2021, doi: 10.1016/j.matlet.2021.130323.

[2] E. J. Duplock, M. Scheffler, and P. J. D. Lindan, "Hallmark of perfect graphene," *Phys Rev Lett*, vol. 92, no. 22, pp. 225502, 2004, doi: 10.1103/PhysRevLett.92.225502.

[3] X. Wang, K. Qu, B. Xu, J. Ren, and X. Qu, "Microwave assisted one-step green synthesis of cell-permeable multicolor photoluminescent carbon dots without surface passivation reagents," *J Mater Chem*, vol. 21, no. 8, pp. 2445–2450, 2011, doi: 10.1039/c0jm02963g.

[4] L. A. Ponomarenko *et al.*, "Chaotic dirac billiard in graphene quantum dots," *Science (1979)*, vol. 320, no. 5874, pp. 356–358, 2008, doi: 10.1126/science.1154663.

[5] L. S. Li and X. Yan, "Colloidal graphene quantum dots," *Journal of Physical Chemistry Letters*, vol. 1, no. 17, pp. 2572–2576, 2010, doi: 10.1021/jz100862f.

[6] F. Yuan *et al.*, "Engineering triangular carbon quantum dots with unprecedented narrow bandwidth emission for multicolored LEDs," *Nat Commun*, vol. 9, no. 1, pp. 2249, 2018, doi: 10.1038/s41467-018-04635-5.

[7] R. Ye *et al.*, "Bandgap engineering of coal-derived graphene quantum dots," *ACS Appl Mater Interfaces*, vol. 7, no. 12, pp. 7041–7048, 2015, doi: 10.1021/acsami.5b01419.

[8] N. Bhatt and M. S. Mehata, "A Sustainable Approach to Develop Gold Nanoparticles with Kalanchoe fedtschenkoi and Their Interaction with Protein and Dye: Sensing and Catalytic Probe," *Plasmonics*, vol. 18, no. 3, pp. 845–858, 2023, doi: 10.1007/s11468-023-01814-z.

[9] S. Zhu, Y. Song, X. Zhao, J. Shao, J. Zhang, and B. Yang, “The photoluminescence mechanism in carbon dots (graphene quantum dots, carbon nanodots, and polymer dots): current state and future perspective,” *Nano Research*, vol. 8, no. 2, pp. 355–381, 2015. doi: 10.1007/s12274-014-0644-3.

[10] M. Bacon, S. J. Bradley, and T. Nann, “Graphene quantum dots,” *Particle and Particle Systems Characterization*, vol. 31, no. 4., pp. 415–428, 2014. doi: 10.1002/ppsc.201300252.

[11] C. Zhao *et al.*, “Synthesis of graphene quantum dots and their applications in drug delivery,” *Journal of Nanobiotechnology*, vol. 18, no. 1, pp.1-32, 2020. doi: 10.1186/s12951-020-00698-z.

[12] M. S. Mehata and S. Biswas, “Synthesis of fluorescent graphene quantum dots from graphene oxide and their application in fabrication of GQDs@AgNPs nanohybrids and sensing of H2O2,” *Ceram Int*, vol. 47, no. 13, pp. 19063–19072, 2021, doi: 10.1016/j.ceramint.2021.03.252.

[13] L. Lu, Y. Zhu, C. Shi, and Y. T. Pei, “Large-scale synthesis of defect-selective graphene quantum dots by ultrasonic-assisted liquid-phase exfoliation,” *Carbon N Y*, vol. 109, pp. 373–383, 2016, doi: 10.1016/j.carbon.2016.08.023.

[14] Z. Fan *et al.*, “Surrounding media sensitive photoluminescence of boron-doped graphene quantum dots for highly fluorescent dyed crystals, chemical sensing and bioimaging,” *Carbon N Y*, vol. 70, pp. 149–156, 2014, doi: 10.1016/j.carbon.2013.12.085.

[15] J. Zhan *et al.*, “A solvent-engineered molecule fusion strategy for rational synthesis of carbon quantum dots with multicolor bandgap fluorescence,” *Carbon N Y*, vol. 130, pp. 153–163, 2018, doi: 10.1016/j.carbon.2017.12.075.

[16] C. Wang *et al.*, “Enhancing Cell Nucleus Accumulation and DNA Cleavage Activity of Anti-Cancer Drug via Graphene Quantum Dots,” *Sci Rep*, vol. 3, no., pp. 2852, 2013, doi: 10.1038/srep02852.

[17] P. Nigam, S. Waghmode, M. Louis, S. Wangnoo, P. Chavan, and D. Sarkar, “Graphene quantum dots conjugated albumin nanoparticles for targeted drug

delivery and imaging of pancreatic cancer," *J Mater Chem B*, vol. 2, no. 21, pp. 3190–3195, 2014, doi: 10.1039/c4tb00015c.

[18] N. A. Travlou, D. A. Giannakoudakis, M. Algarra, A. M. Labella, E. Rodríguez-Castellón, and T. J. Bandosz, "S- and N-doped carbon quantum dots: Surface chemistry dependent antibacterial activity," *Carbon N Y*, vol. 135, pp. 104–111, 2018, doi: 10.1016/j.carbon.2018.04.018.

[19] J. Ge *et al.*, "A graphene quantum dot photodynamic therapy agent with high singlet oxygen generation," *Nat Commun*, vol. 5, pp. 4596, 2014, doi: 10.1038/ncomms5596.

[20] A. Ananthanarayanan *et al.*, "Facile synthesis of graphene quantum dots from 3D graphene and their application for Fe3+ sensing," *Adv Funct Mater*, vol. 24, no. 20, pp. 3021–3026, 2014, doi: 10.1002/adfm.201303441.

[21] F. Niu, Y. L. Ying, X. Hua, Y. Niu, Y. Xu, and Y. T. Long, "Electrochemically generated green-fluorescent N-doped carbon quantum dots for facile monitoring alkaline phosphatase activity based on the Fe3+-mediating ON-OFF-ON-OFF fluorescence principle," *Carbon N Y*, vol. 127, no. pp. 340–348, 2018, doi: 10.1016/j.carbon.2017.10.097.

[22] V. Wood *et al.*, "Inkjet-printed quantum dot-polymer composites for full-color AC-driven displays," *Advanced Materials*, vol. 21, no. 21, pp. 2151–2155, 2009, doi: 10.1002/adma.200803256.

[23] H. Li *et al.*, "Water-soluble fluorescent carbon quantum dots and photocatalyst design," *Angewandte Chemie - International Edition*, vol. 49, no. 26, pp. 4430–4434, 2010, doi: 10.1002/anie.200906154.

[24] L. Malfatti and P. Innocenzi, "Sol-Gel Chemistry for Carbon Dots," *Chemical Record*, vol. 18, no. 7, pp. 1192–1202, 2018. doi: 10.1002/tcr.201700108.

[25] M. Ma, X. Hu, C. Zhang, C. Deng, and X. Wang, "The optimum parameters to synthesize bright and stable graphene quantum dots by hydrothermal method," *Journal of Materials Science: Materials in Electronics*, vol. 28, no. 9, pp. 6493–6497, 2017, doi: 10.1007/s10854-017-6337-4.

[26] M. He, X. Guo, J. Huang, H. Shen, Q. Zeng, and L. Wang, “Mass production of tunable multicolor graphene quantum dots from an energy resource of coke by a one-step electrochemical exfoliation,” *Carbon N Y*, vol. 140, pp. 508–520, 2018, doi: 10.1016/j.carbon.2018.08.067.

[27] R. L. Calabro, D. S. Yang, and D. Y. Kim, “Liquid-phase laser ablation synthesis of graphene quantum dots from carbon nano-onions: Comparison with chemical oxidation,” *J Colloid Interface Sci*, vol. 527, pp. 132–140, 2018, doi: 10.1016/j.jcis.2018.04.113.

[28] K. Habiba, V. I. Makarov, J. Avalos, M. J. F. Guinel, B. R. Weiner, and G. Morell, “Luminescent graphene quantum dots fabricated by pulsed laser synthesis,” *Carbon N Y*, vol. 64, pp. 341–350, 2013, doi: 10.1016/j.carbon.2013.07.084.

[29] L. M. Dong, D. Y. Shi, Z. Wu, Q. Li, and Z. D. Han, “IMPROVED SOLVOTHERMAL METHOD FOR CUTTING GRAPHENE OXIDE INTO GRAPHENE QUANTUM DOTS,” Digest Journal of Nanomaterials and Biostructures, vol. 10, pp. 855-864, 2015.

[30] A. Abbas, T. A. Tabish, S. J. Bull, T. M. Lim, and A. N. Phan, “High yield synthesis of graphene quantum dots from biomass waste as a highly selective probe for Fe3+ sensing,” *Sci Rep*, vol. 10, no. 1, 2020, doi: 10.1038/s41598-020-78070-2.

[31] D. K. Ray, N. Ramankutty, N. D. Mueller, P. C. West, and J. A. Foley, “Recent patterns of crop yield growth and stagnation,” *Nat Commun*, vol. 3, pp. 1293, 2012, doi: 10.1038/ncomms2296.

[32] T. Jorn-am, J. Praneerad, R. Attajak, N. Sirisit, J. Manyam, and P. Paoprasert, “Quasi-solid, bio-renewable supercapacitor with high specific capacitance and energy density based on rice electrolytes and rice straw-derived carbon dots as novel electrolyte additives,” *Colloids Surf A Physicochem Eng Asp*, vol. 628, pp. 127239, 2021, doi: 10.1016/j.colsurfa.2021.127239.

[33] W. Wang, J. C. Martin, X. Fan, A. Han, Z. Luo, and L. Sun, "Silica nanoparticles and frameworks from rice husk biomass," *ACS Appl Mater Interfaces*, vol. 4, no. 2, pp. 977–981, 2012, doi: 10.1021/am201619u.

[34] Z. Wang *et al.*, "Large-Scale and Controllable Synthesis of Graphene Quantum Dots from Rice Husk Biomass: A Comprehensive Utilization Strategy," *ACS Appl Mater Interfaces*, vol. 8, no. 2, pp. 1434–1439, 2016, doi: 10.1021/acsami.5b10660.

[35] W. Wang, J. C. Martin, N. Zhang, C. Ma, A. Han, and L. Sun, "Harvesting silica nanoparticles from rice husks," *Journal of Nanoparticle Research*, vol. 13, no. 12, pp. 6981–6990, 2011, doi: 10.1007/s11051-011-0609-3.

[36] N. Liu, K. Huo, M. T. McDowell, J. Zhao, and Y. Cui, "Rice husks as a sustainable source of nanostructured silicon for high performance Li-ion battery anodes," *Sci Rep*, vol. 3, pp. 1919, 2013, doi: 10.1038/srep01919.

[37] C. Real, M. D. Alcala, and J. M. Criado, "Synthesis of Silicon Nitride from Carbothermal Reduction of Rice Husks by the Constant-Rate-Thermal-Analysis (CRTA) Method," J. am. Ceram. Soc., vol. 87, pp. 75-78, 2004.

[38] E. P. Ng, H. Awala, K. H. Tan, F. Adam, R. Retoux, and S. Mintova, "EMT-type zeolite nanocrystals synthesized from rice husk," *Microporous and Mesoporous Materials*, vol. 204, pp. 204–209, 2015, doi: 10.1016/j.micromeso.2014.11.017.

[39] W. Huang *et al.*, "Induction of Bilirubin Clearance by the Constitutive Androstane Receptor (CAR)," proc. Natl. acad. Sci. vol.100, pp. 4156-4161, 2003.

[40] C. Greco *et al.*, "Neonatal Jaundice in Low- and Middle-Income Countries: Lessons and Future Directions from the 2015 Don Ostrow Trieste Yellow Retreat," *Neonatology*, vol. 110, no. 3, pp. 172–180, 2016. doi: 10.1159/000445708.

[41] S. Oza, J. E. Lawn, D. R. Hogan, C. Mathers, and S. N. Cousens, "Estimations des causes de décès néonatales pour les périodes néonatales précoces et

tardives dans 194 pays: 2000–2013," *Bull World Health Organ*, vol. 93, no. 1, pp. 19–28, 2015, doi: 10.2471/BLT.14.139790.

[42] K. Kurosaka, S. Senba, H. Tsubota, and H. Kondo, "A new enzymatic assay for selectively measuring conjugated bilirubin concentration in serum with use of bilirubin oxidase," clinica chimica acta, vol. 269, pp.125-136,1998.

[43] J. Wang, D. B. Luo, and P. M. Farias, "DETERMINATION OF BlLIRUBIN BY ADSORPTIVE STRIPPING VOETAlblMETRY Chmcal laboratones measure btibm spectrophotometncally, either chrectly OF after a dlazo," J Electroanal Chem, vol. 185, pp. 61-71, 1985.

[44] K. Shanmugaraj and S. A. John, "Water-soluble MoS2 quantum dots as effective fluorescence probe for the determination of bilirubin in human fluids," *Spectrochim Acta A Mol Biomol Spectrosc*, vol. 215, pp. 290–296, May 2019, doi: 10.1016/j.saa.2019.02.104.

[45] Z. Yang, J. Yan, and C. Zhang, "Piezoelectric detection of bilirubin based on bilirubin-imprinted titania film electrode," *Anal Biochem*, vol. 421, no. 1, pp. 37–42, 2012, doi: 10.1016/j.ab.2011.10.027.

[46] C. Lu, J. M. Lin, and C. W. Huie, "Determination of total bilirubin in human serum by chemiluminescence from the reaction of bilirubin and peroxynitrite," *Talanta*, vol. 63, no. 2, pp. 333–337, 2004, doi: 10.1016/j.talanta.2003.10.049.

[47] P. Kannan, H. Chen, V. T. W. Lee, and D. H. Kim, "Highly sensitive amperometric detection of bilirubin using enzyme and gold nanoparticles on sol-gel film modified electrode," *Talanta*, vol. 86, no. 1, pp. 400–407, 2011, doi: 10.1016/j.talanta.2011.09.034.

[48] O. S. Wolfbeis, "An overview of nanoparticles commonly used in fluorescent bioimaging," *Chemical Society Reviews*, vol. 44, no. 14, pp. 4743–4768, 2015. doi: 10.1039/c4cs00392f.

[49] M. H. M. Facure, R. Schneider, L. A. Mercante, and D. S. Correa, "A review on graphene quantum dots and their nanocomposites: From laboratory synthesis towards agricultural and environmental applications,"

Environmental Science: Nano, vol. 7, no. 12, pp. 3710–3734, 2020. doi: 10.1039/d0en00787k.

[50] A. K. Chaturvedi, A. Pappu, and M. K. Gupta, "Unraveling the role of agro waste-derived graphene quantum dots on dielectric and mechanical property of the fly ash-based polymer nanocomposite," *J Alloys Compd*, vol. 903, pp. 163953, 2022, doi: 10.1016/j.jallcom.2022.163953.

[51] R. S. Dubey, Y. B. R. D. Rajesh, and M. A. More, "Synthesis and Characterization of SiO2 Nanoparticles via Sol-gel Method for Industrial Applications," in *Materials Today: Proceedings*, Elsevier Ltd, vol. 2, pp. 3575–3579, 2015. doi: 10.1016/j.matpr.2015.07.098.

[52] W. Wang *et al.*, "One-pot Facile Synthesis of Graphene Quantum Dots from Rice Husks for Fe 3+ Sensing." ACS, vol. 57, pp. 1-15, 2018.

[53] S. S. Ibrahim, H. H. Elbehery, and A. Samy, "The efficacy of green silica nanoparticles synthesized from rice straw in the management of Callosobruchus maculatus (Col., Bruchidae)," *Sci Rep*, vol. 14, no. 1, 2024, doi: 10.1038/s41598-024-58856-4.

[54] A. Abbas, Q. Liang, S. Abbas, M. Liaqat, S. Rubab, and T. A. Tabish, "Eco-Friendly Sustainable Synthesis of Graphene Quantum Dots from Biowaste as a Highly Selective Sensor," *Nanomaterials*, vol. 12, no. 20, pp. 3696, 2022, doi: 10.3390/nano12203696.

[55] A. Abbas, T. A. Tabish, S. J. Bull, T. M. Lim, and A. N. Phan, "High yield synthesis of graphene quantum dots from biomass waste as a highly selective probe for Fe3+ sensing," *Sci Rep*, vol. 10, no. 1, pp. 21262, 2020, doi: 10.1038/s41598-020-78070-2.

[56] J. Tauc, R. Grigorovici, and A. Vancu, "J. TAUC et al: Optical Properties and Electronic Structure of Ge Optical Properties and Electronic Structure of Amorphous Germanium," phys. stat. sol., vol. 15, pp. 627-637, 1966.

[57] S. He, M. J. Turnbull, Y. Nie, X. Sun, and Z. Ding, "Band structures of blue luminescent nitrogen-doped graphene quantum dots by synchrotron-based XPS," *Surf Sci*, vol. 676, pp. 51–55, 2018, doi: 10.1016/j.susc.2018.01.013.

[58] Y. N. Hao, H. L. Guo, L. Tian, and X. Kang, “Enhanced photoluminescence of pyrrolic-nitrogen enriched graphene quantum dots,” *RSC Adv*, vol. 5, no. 54, pp. 43750–43755, 2015, doi: 10.1039/c5ra07745a.

[59] L. L. Li *et al.*, “A facile microwave avenue to electrochemiluminescent two-color graphene quantum dots,” *Adv Funct Mater*, vol. 22, no. 14, pp. 2971–2979, 2012, doi: 10.1002/adfm.201200166.

[60] A. Ananthanarayanan *et al.*, “Facile synthesis of graphene quantum dots from 3D graphene and their application for Fe3+ sensing,” *Adv Funct Mater*, vol. 24, no. 20, pp. 3021–3026, 2014, doi: 10.1002/adfm.201303441.

[61] A. Suryawanshi *et al.*, “Large scale synthesis of graphene quantum dots (GQDs) from waste biomass and their use as an efficient and selective photoluminescence on-off-on probe for Ag+ ions,” *Nanoscale*, vol. 6, no. 20, pp. 11664–11670, 2014, doi: 10.1039/c4nr02494j.

[62] A. C. Croce, A. Ferrigno, G. Santin, M. Vairetti, and G. Bottiroli, “Bilirubin: An autofluorescence bile biomarker for liver functionality monitoring,” *J Biophotonics*, vol. 7, no. 10, pp. 810–817, 2014, doi: 10.1002/jbio.201300039.

[63] M. S. Mehata, “An efficient excited-state proton transfer fluorescence quenching based probe (7-hydroxyquinoline) for sensing trivalent cations in aqueous environment,” *J Mol Liq*, vol. 326, 2021, doi: 10.1016/j.molliq.2021.115379.

[64] V. Sharma and M. S. Mehata, “Rapid optical sensor for recognition of explosive 2,4,6-TNP traces in water through fluorescent ZnSe quantum dots,” *Spectrochim Acta A Mol Biomol Spectrosc*, vol. 260, 2021, doi: 10.1016/j.saa.2021.119937.

[65] H. Kumar and S. Obrai, “Highly sensitive and selective detection of free bilirubin using blue emitting graphene quantum dots (GQDs)”, J chem. Sci., vol. 134, pp. 85, 2022, doi: 10.1007/s12039-022.

APPENDIX I

Similarity Report

PAPER NAME
THESIS BODY.docx

WORD COUNT **3760 Words**	CHARACTER COUNT **20835 Characters**
PAGE COUNT **30 Pages**	FILE SIZE **7.4MB**
SUBMISSION DATE **Jun 6, 2024 6:44 PM GMT+5:30**	REPORT DATE **Jun 6, 2024 6:45 PM GMT+5:30**

8% Overall Similarity

The combined total of all matches, including overlapping sources, for each database.

- 4% Internet database
- 3% Publications database
- Crossref database
- Crossref Posted Content database
- 6% Submitted Works database

Excluded from Similarity Report

- Bibliographic material
- Quoted material
- Cited material
- Small Matches (Less then 8 words)

Summary

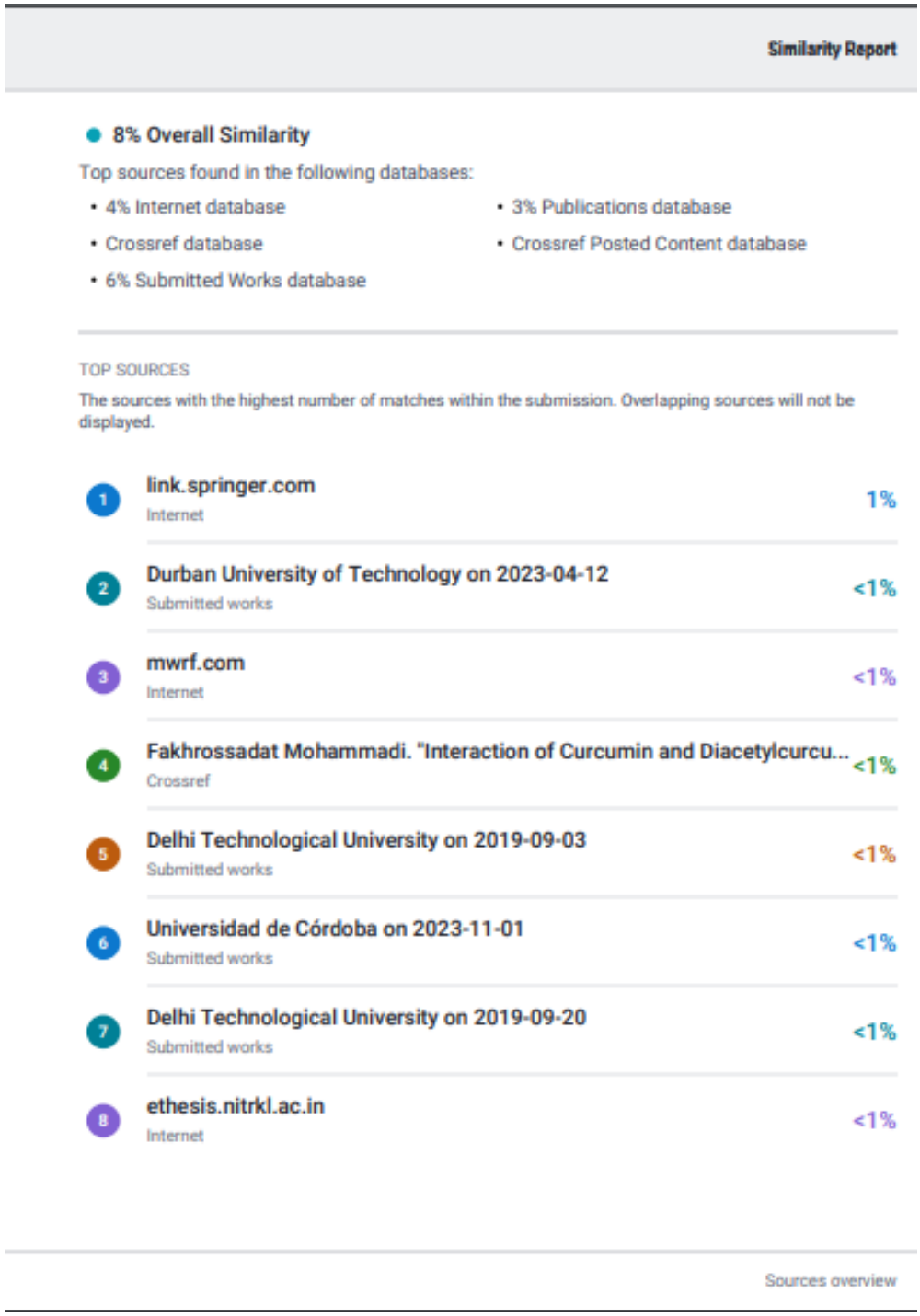

Similarity Report

8% Overall Similarity

Top sources found in the following databases:

- 4% Internet database
- 3% Publications database
- Crossref database
- Crossref Posted Content database
- 6% Submitted Works database

TOP SOURCES

The sources with the highest number of matches within the submission. Overlapping sources will not be displayed.

1	link.springer.com Internet	1%
2	Durban University of Technology on 2023-04-12 Submitted works	<1%
3	mwrf.com Internet	<1%
4	Fakhrossadat Mohammadi. "Interaction of Curcumin and Diacetylcurcu... Crossref	<1%
5	Delhi Technological University on 2019-09-03 Submitted works	<1%
6	Universidad de Córdoba on 2023-11-01 Submitted works	<1%
7	Delhi Technological University on 2019-09-20 Submitted works	<1%
8	ethesis.nitrkl.ac.in Internet	<1%

Sources overview

Similarity Report

9	nature.com Internet	<1%
10	pubfacts.com Internet	<1%
11	Universiti Teknologi Malaysia on 2017-06-02 Submitted works	<1%
12	Universiti Tunku Abdul Rahman on 2014-05-13 Submitted works	<1%
13	dro.dur.ac.uk Internet	<1%
14	jesc.ac.cn Internet	<1%
15	Aston University on 2020-06-30 Submitted works	<1%
16	Chuang Han, Nan Zhang, Yi-Jun Xu. "Structural diversity of graphene m... Crossref	<1%
17	Chulalongkorn University on 2013-09-03 Submitted works	<1%
18	Durban University of Technology on 2022-12-26 Submitted works	<1%
19	Kourosh Rahimi, Ahmad Yazdani, Mohammad Ahmadirad. "Facile prep... Crossref	<1%
20	Mohamed, M.M.. "Characterization, adsorption and photocatalytic acti... Crossref	<1%

Sources overview

Similarity Report

21	University of Florida on 2022-04-26 Submitted works	<1%
22	scholarbank.nus.edu.sg Internet	<1%

APPENDIX II

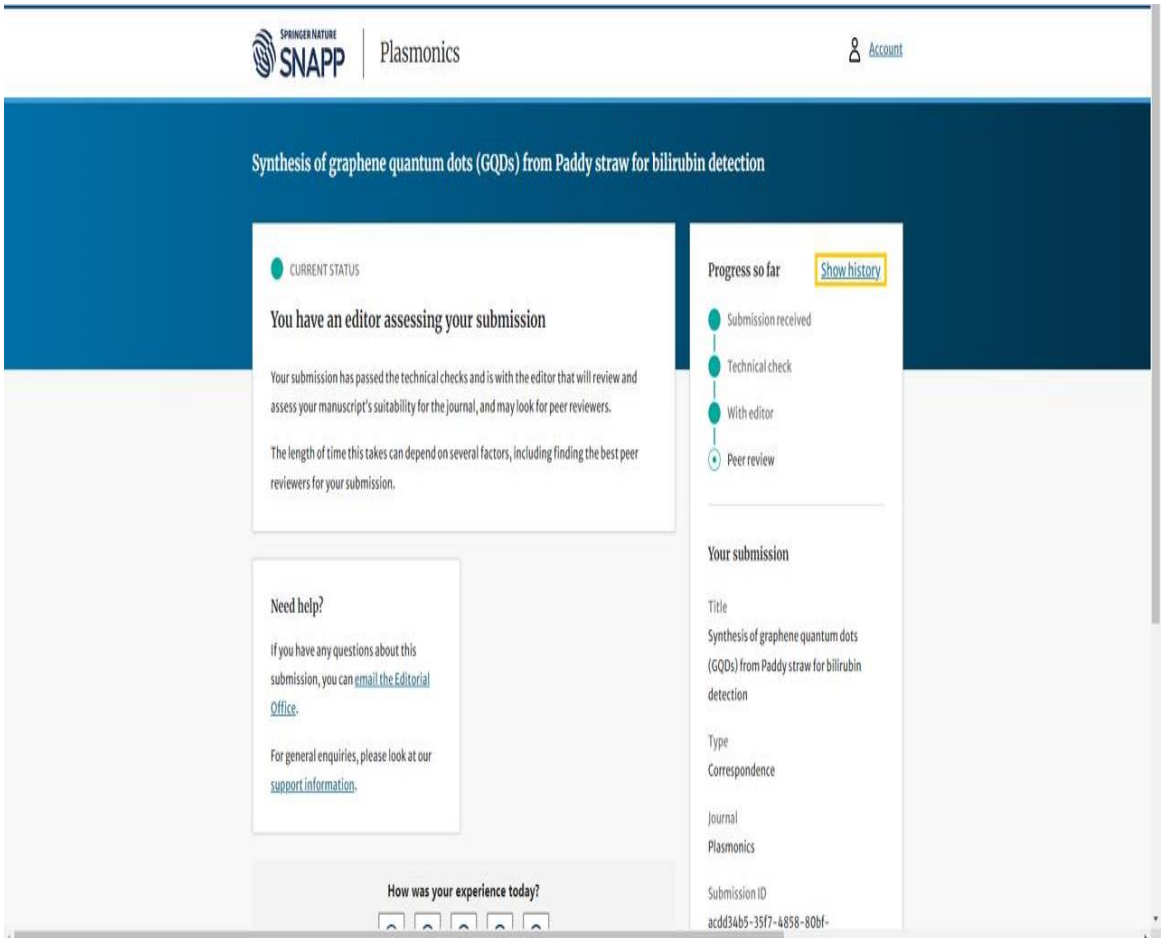
SPRINGER NATURE
SNAPP
Plasmonics
Account
Synthesis of graphene quantum dots (GQDs) from Paddy straw for bilirubin detection
CURRENT STATUS
You have an editor assessing your submission
Your submission has passed the technical checks and is with the editor that will review and assess your manuscript's suitability for the journal, and may look for peer reviewers.
The length of time this takes can depend on several factors, including finding the best peer reviewers for your submission.
Need help?
If you have any questions about this submission, you can email the Editorial Office.
For general enquiries, please look at our support information.
How was your experience today?
Progress so far
Show history
Submission received
Technical check
With editor
Peer review
Your submission
Title
Synthesis of graphene quantum dots (GQDs) from Paddy straw for bilirubin detection
Type
Correspondence
Journal
Plasmonics
Submission ID
acdd34b5-35f7-4858-80bf-

From: Plasmonics shaina.sunga@springernature.com
Subject: Plasmonics: Decision on your manuscript
Date: 6 Jun 2024 at 10:14:51 PM
To: msmehata@gmail.com

Ref: Submission ID acdd34b5-35f7-4858-80bf-01630fc90c41

Dear Dr Mehata,

Re: "Synthesis of graphene quantum dots (GQDs) from Paddy straw for bilirubin detection"

We're delighted to let you know that your manuscript has been accepted for publication in Plasmonics.

Prior to publication, our production team will check the format of your manuscript to ensure that it conforms to the journal's requirements. They will be in touch shortly to request any necessary changes, or to confirm that none are needed.

Checking the proofs

Once we've prepared your paper for publication, you will receive a proof. At this stage, for the main text, only errors that have been introduced during the production process, or those that directly compromise the scientific integrity of the paper, may be corrected.

As the corresponding (or nominated) author, you are responsible for the accuracy of all content, including spelling of names and current affiliations.

To ensure prompt publication, your proofs should be returned within two working days.

Publication policies

Acceptance of your manuscript is conditional on all authors agreeing to our publication policies at: https://www.springernature.com/gp/policies/editorial-policies

Plasmonics is a hybrid journal. This means when the journal accepts research for publication, the article may be published using either immediate gold open access or the subscription publishing route. For further information please visit https://www.springernature.com/gp/open-research/about/green-or-gold-routes-to-OA/hybrid-options

Once again, thank you for choosing Plasmonics, and we look forward to publishing your article.

Kind regards,

Chris Geddes
Editor
Plasmonics